Iodine chemistry in the + 1 oxidation state. II. A Raman and uv-visible spectroscopic study of the disproportionation of hypoiodite in basic solutions'

J. C. WREN, J. PAQUETTE, S. SUNDER, AND B. L. FORD

Research Chemistry Branch, Atomic Energy of Canada Limited, Whiteshell Nuclear Research Establishment, Pinawa, Man., Canada ROE 1 LO

Received March 14, 1986

J. C. WREN, J. PAQUETTE, S. SUNDER, and B. L. FORD. Can. J. Chem. 64, 2284 (1986).

The kinetics of disproportionation of elemental iodine to iodide and iodate ions has been studied in basic aqueous media using Raman and uv-visible spectroscopy. The IO stretching vibrations for IO- and I_2OH^- were observed at 430 ± 2 and 560 ± 2 cm-', respectively. The totally symmetric stretching vibration for IO_2^- was observed at 685 ± 2 cm-'. The Raman results indicate that I_2OH^- is a linear molecule with a stronger 1-O bond rhan IO^-. The rare expression at 25°C in 1 mol dm^{-3} NaOH was found to be

$$-\frac{d\Sigma[I]}{dt} = (0.05 + 2.60[I^-])(\Sigma[I])^2$$

where

$$\Sigma[I] = ([I_2] + [I;] + [IO-] + [I_2OH^-])$$

The reaction is primarily a reaction of the iodine + 1 oxidation-state species IO- and I_2OH^-. It proceeds through the + 3 oxidation-state species IO_2^-. The following equilibrium and rate constants were determined:

$IO- + I^- + H_2O \rightleftharpoons I_2OH^- + OH^-$	$K = 0.15 \pm 0.01$
$IO^- + IO^- \rightarrow 10; + I^-$	$k \leq 7.2 \times 10^{-2}$ dm^3 mol^{-1} s^{-1}
$IO- + HOI + IO; + I- + H+$	$k = 40 \pm 7$ dm^3 mol^{-1} s^{-1}
$IO- + I_2OH^- \rightarrow IO; + 2I^- + H+$	$k = 6.0 \pm 0.2$ dm^3 mol^{-1} s^{-1}
$IO^- + 10; \rightarrow IO_3^- + I^-$	$k = 0.5 \pm 0.1$ dm^3 mol^{-1} s^{-1}
$I_2OH^- + IO, \rightarrow IO_3^- + 2I^- + H+$	$k = 26 \pm 2$ dm^3 mol^{-1} s^{-1}

J. C. WREN, J. PAQUETTE, S. SUNDER et B. L. FORD. Can. J. Chem. 64, 2284 (1986).

La cinétique de dismutation de l'iode en ions iodure et iodate a été étudiée en milieu aqueux basique, en utilisant la spectroscopie Raman et UV-visible. La vibration d'tlongation pour IO- et I_2OH^- a été observte à 430 ± 2 et 560 ± 2 cm-', respectivement. **La vibration d'élongation totalement symétrique pour IO_2^- a été observée à 685 ± 2 cm-'. Les résultats de la** spectroscopie Ràman indiquent que I_2OH^- est une molécule lintaire avec un lien I-O plus fort que dans IO-. La loi cinttique à 25°C, en milieu NaOH 1 mol dm^{-3}, est

$$-\frac{d\Sigma[I]}{dt} = (0.05 + 2.60[I^-])(\Sigma[I])^2$$

où

$$\Sigma[I] = ([I_2] + [I_3^-] + [IO-] + [I_2OH^-])$$

La reaction est principalement une reaction de l'iode dans l'état d'oxydation + 1 et implique les espèces IO^- et I_2OH^-. L'iode dans l'état d'oxydation + 3, sous forme de IO_2^-, est un intermédiaire réactif. Les constantes d'équilibre et de vitesse suivantes ont été mesurées :

$IO- + I- + H_2O \rightleftharpoons I_2OH^- + OH-$	$K = 0,15 \pm 0,01$
$IO- + IO^- \rightarrow IO_2^- + I^-$	$k \leq 7.2 \times 10^{-2}$ dm^3 mol^{-1} s^{-1}
$IO^- + HOI \rightarrow IO_2^- + I^- + H^+$	$k = 40 \pm 7$ dm^3 mol^{-1} s^{-1}
$IO- + I_2OH^- \rightarrow IO; + 2I^- + H+$	$k = 6,0 \pm 0,2$ dm^3 mol^{-1} s^{-1}
$IO^- + IO_2^- \rightarrow IO_3^- + I^-$	$k = 0,5 \pm 0,1$ dm^3 mol^{-1} s^{-1}
$I_2OH^- + IO; \rightarrow IO; + 2I^- + H+$	$k = 26 \pm 2$ dm^{3}mol^{-1}s^{-1}

I. Introduction

The disprnportionation of elemental iodine into iodide and iodate ions is a key reaction controlling the behaviour of iodine in aqueous media:

[1] $3I_2 + 3H_2O \rightleftharpoons 5I^- + IO; + 6H^+$

'AECL No. 9037.

The thermodynamic parameters for equilibrium [1] are known accurately for temperatures up to 150°C (1). The kinetics of the reverse reaction (Dushman reaction) have also been examined in detail (2–4), but the forward reaction has not been studied so extensively. Thomas et al. (5) have investigated its kinetics in neutral to weakly basic media, while other studies (6–11) have been performed in strongly basic media. These authors agree

that the rate-determining step involves the reactions of the + 1 oxidation-state species HOI/IO-, the hydrolysis and disproportionation of elemental iodine into HOI/IO- and I^- being a rapid process. However, there is disagreement in the suggested rate laws for further disproportionation to iodide and iodate. Skrabal (9, 10) and Forster (11), as well as Li and White (8), have reported a two-term rate law, with the second term having a first-order dependence on iodide concentration, an effect not observed in the more recent studies of Thomas *et al.* (5) and Haimovich and Treinin (6).

Although some of these studies were done using uv-visible absorption spectroscopy (5, 6), the transient iodine species have never been positively identified. There is no report in the literature on the Raman spectra of any of the intermediates formed during the disproportionation of iodine. For these reasons, we have used the following three reactions to study the kinetics of disproportionation of iodine in basic media, using both Raman and uv-visible spectroscopy:

[2] $I_2 + OH^- \rightleftharpoons IO^- + I^- + H^+$

[3] $HOCl + I^- \rightleftharpoons IO^- + Cl^- + H^+$

[4] $ICl + OH^- \rightleftharpoons IO^- + Cl^- + H^+$

Using Raman spectroscopy, we not only observed the transient iodine species, but also obtained reliable kinetic data for the reaction of these species. We also reinvestigated the kinetics using uv-visible spectrophotometry and iodide-specific electrode measurements to obtain accurate values of the rate constants.

Our interest in aqueous iodine chemistry arises from the importance of iodine compounds in nuclear reactor safety studies. Radioactive isotopes of iodine are among the more radiologically toxic products resulting from the fission of uranium. A knowledge of the aqueous chemistry of iodine is needed to design effective measures to prevent the release of volatile radioactive iodine species into the environment following a serious nuclear reactor accident.

II. Experimental

Reagents

The sodium iodide was of ACS grade and was used without further purification. The hypochlorite was either obtained as a stock solution from the Fisher Scientific Company or generated hy slowly bubbling chlorine gas, from Canadian Liquid Air, into a cold 1 mol dm^{-3} NaOH solution. The iodine was resublimed ACS grade and was used as such. The iodine monochloride was obtained from the J. T. Baker Chemical Company and was used as received. Other stock solutions were prepared from ACS-grade chemicals and distilled deionized water.

The experiments at low initial iodide concentration were performed using an ICl_2^- stock solution. prepared by dissolving ICl(s) in 1 mol dm^{-3} HCl. The concentration of the stock ICl_2^- solution was determined from its light absorption at 345 nm (ϵ_{max} = 243 $dm^3\ mol^{-1}\ cm^{-1}$) (12).

The effect of iodide concentration was studied using I_2/I^- solutions prepared by dissolving I_2 in solutions containing various NaI concentrations. For the Raman studies, the I_2 concentration was fixed at 0.1 mol dm^{-3}, and the I^- concentration varied between 0.2 and 2 mol dm^{-3}. Some experiments were performed with added NaCl, to study the effect of the ionic strength. For the uv-visible spectrophotometric experiments, the I_2 concentration was fixed at 0.01 mol dm^{-3} and the I^- concentration varied between 0. 1 and I mol dm^{-3}; the NaCl concentration was adjusted to provide a constant ionic strength of 1.5 mol dm^{-3}.

For the Raman studies at lower pH (12.0 and 10.5), 0.1 mol dm^{-3} OCl^- and 0.1 mol dm^{-3} I^- solutions were used, in borax buffer for a pH value of 12, and in phosphate buffer for a pH value of 10.5. The hypochlorite stock solutions were analyzed by titration with NaI in 0.01 mol dm^{-3} H_2SO_4, using an Orion iodide-specific electrode (Model 94-53) and an Orion double-junction reference electrode (Model 90-02) as an end-point indicator. The OCl^- absorption band at 290 nm (ϵ = 350 $dm^3\ mol^{-1}\ cm^{-1}$) was also used to analyze for hypochlorite.

Raman spectroscopy

The Raman spectra were obtained using a SPEX 1403 double monochromator equipped with two 1800 grooves/mm gratings, a SPEX 1459 uv-visible illuminator, a RCA C-31034 photomultiplier tube, and photon counting electronics. The spectrometer operates under the control of a SPEX-DATAMATE microcomputer system. The frequency scale was calibrated using the emission lines of a mercury lamp and the ν_1 band of liquid carbon tetrachloride. Most of the Raman spectra were excited using the 514.5-nm radiation from a Spectra-Physics Model 165-09 argon-ion laser. Some of the spectra were also excited with the 488.0-nm radiation, but no difference in the results could be noticed. The laser power at the sample was about 900 mW and the spectra were recorded at a spectral band pass of about 6 cm^{-1}.

The kinetic runs for Raman studies were initiated either by reacting I_2/I^- solutions with an equal volume of a 2 mol dm^{-3} NaOH solution (reaction [2]) or, at pH values of 12 and 10.5, by reacting a 0.1 mol dm^{-3} OCl^- solution with an equal volume of a 0.1 mol dm^{-3} I^- solution (reaction [3]). A flow system was used to observe the Raman spectra of the transient iodine species so obtained. The two reactant solutions were driven by a double-syringe pump into a small Plexiglass mixing chamber. The reacting mixture then travelled down a length of Tygon tubing attached to a tine glass capillary, producing a stable stream of solution in the open air in the sample compartment of the Raman spectrometer. The laser beam was focussed on a point in the stream, about 3 mm from the tip of the glass capillary. Flow rates of the order of 0.1 $cm^3\ s^{-1}$ were used. The spectra of the transient iodine species could be observed at various reaction times by changing the length of the Tygon tubing. The above procedure was necessary since bands due to glass, quartz, or sapphire were found to interfere with the spectra of the transient iodine species. This technique not only removed the extraneous bands, but also enhanced the observed Raman intensities by a factor of about ten compared with those obtained using a glass capillary. The experiments were performed at room temperature (22 ± IT).

Each spectrum was obtained by averaging at least five scans from the 300- to 900-cm-' region and subtracting the average background spectra. The background spectra were obtained with a solution containing the same concentration of I^- and NaOH, but without I_2. For the studies done at pH values of 12 and 10.5, the background spectra were obtained with 0.05 mol dm^{-3} I^- in the appropriate buffer solution. Spectra from 50 to 300 cm- ^{1} (ν_1 of I_3^- and I_2) and from 2800 to 3800 cm^{-1} (ν_{OH} of H_2O) were also recorded for each run. To compensate for any variation in the optical alignment or laser power, the intensities of the various Raman bands were normalized using the water band (OH stretching vibration) as an internal standard.

Ultraviolet-visible spectrophotometry

The uv-visible spectra were recorded in digital form using a double-beam diode-array spectrophotometer (Hewlett-Packard 8450A) interfaced to a Hewlett-Packard HP-85 microcomputer via a HP-82939h serial interface. Some experiments were also performed using a Cary-17D spectrophotometer interfaced to the HP-85 microcomputer via a HP-82941A BCD interface. The temperature was maintained at 25.0 ± 0.1°C using a recirculating water bath

Kinetic runs at low iodide concentration were initiated by injecting, with a glass syringe, 1 mL of a NaOH solution into a 1-cm pathlength spectrophotometric cell containing an equal volume of an ICl^-_2/HCl solution (reaction [4]). A NaOH/NaCl solution was used as the reference. The spectrum between 240 and 500nm was recorded as

a function of time for at least two half-lives. Due to the heat of neutralization, the temperature rose by about 5°C at mixing time; however, the temperature returned to 25.0 ± 0.2°C within 45 s. Since the half-reaction times are of the order of 3000 s, the results were unaffected by the initial temperature transient.

Kinetic runs to study the effect of iodide concentration were initiated by injecting, with a glass syringe, a NaOH solution into an equal volume of an I_2/I^-/NaCl solution contained in a 1-cm pathlength spectrophotometric cell (reaction [2]). A NaOH/I^-/NaCl solution was used as the reference. The absorbance at 363 nm was recorded as a function of time for at least two half-lives.

Iodide-specific electrode

The iodide concentrations were measured with an iodide-specific electrode (Orion 95-53) and a double-junction reference electrode (Orion 90-02) coupled to an Orion Model 701A ionalyzer. The electrode system was calibrated with standard NaI solutions in 1 mol dm^{-3} NaOH, using a 1 mol dm^{-3} NaOH solution in the outer chamber of the double-junction reference electrode. The iodide concentration was calculated from the potential of the electrode system using the relation

$$[5] \quad E = E^0 + B \log_{10} [I^-]$$

where E^0 is a constant that depends on the electrode system, B is the Nemst constant, and E is the measured potential. The experimental value of B, obtained in the I^- concentration range 10^{-2} to 10^{-4} mol dm^{-3}, agreed well with the theoretical value of 59.2 mV at 25°C.

III. Results

Raman spectroscopy

Reaction of I_2/I^-

Figure 1 shows the Raman spectra obtained by reacting an I_2(0.1 mol dm^{-3})/I^-(0.6 mol dm^{-3}) solution with an equal volume of a 2 mol dm^{-3} NaOH solution (reaction [2]). The spectrum of the unreacted I_2/I^- solution showed Raman bands due to I_2 and I_3^-, as expected, including the ν_1 fundamental of I_2 at ~212 cm-' and the ν_1 fundamental of I_3^- at 11.5 ± 2 cm^{-1}, as well as the overtones of I_3^- ($2\nu_1$ at 235 ± 4, $3\nu_1$ at 352 ± 2, and $4\nu_1$ at 465 ± 2 cm-^{1}) (13). These bands disappeared on mixing, as two new bands, not present in the spectra of the reactants, appeared at 430 and 560 cm^{-1} immediately after mixing. After a short time, bands at 685 and 800 cm-' could also be seen. At long reaction times, the spectra showed only one band at 800 cm-'. The intensity of the 430- and 560-cm^{-1} bands decreased steadily with time, although the I_{560}/I_{430} ratio, where I, is the Raman intensity at frequency ν, remained constant throughout the reaction. The intensity of 685-cm^{-1} band increased from zero at short reaction time, went through a maximum, and then decayed to zero at long reaction times. The intensity of the 800-cm^{-1} band, which was initially zero, increased with time but levelled off at long reaction times.

Changing the initial I^- concentration at constant I_2 and OH^- concentrations affected the relative intensity of the 430- and 560-cm^{-1} bands, as well as the time behaviour of all four bands. Although the I_{560}/I_{430} ratio was constant as a function of time for a fixed concentration of I, its value increased linearly with the iodide ion concentration, as can be seen from Fig. 2(a). Figure 2(b) shows that the intensity of the 430-cm-' band at mixing time decreased slightly with an increase in I^- concentration, whereas the intensity of the 560-cm^{-1} band at mixing time increased markedly with an increase in I^- concentration.

Plots of the inverse of the Raman intensities at 560 and 430 cm^{-1} as a function of reaction time for various initial iodide concentrations showed linear relationships (see Fig. 3), indicating that the species responsible for the Raman scattering at 560 and 430 cm^{-1} were decaying by a second-order process. For a second-order process, the slope is k'_ν/α_ν and the intercept is $(\alpha_\nu C^0_\nu)^{-1}$. Here k'_ν, α_ν, and C^0_ν are the apparent second-order rate constant, the Raman scattering probability, and the initial concentration of the species responsible for the Raman band at frequency v. respectively. The k'_{560}/α_{560} and k'_{430}/α_{430} values are plotted as a function of iodide concentration in Fig. 4. The k'_{560}/α_{560} ratio decreases slightly with an increase in iodide concentration, whereas k'_{430}/α_{430} increases with the iodide concentration. Thus, the rate of decay of the species responsible for the Raman scattering at 560 cm-' is second order in that species and close to zero order in iodide, whereas the rate of decay of the species responsible for the Raman scattering at 430 cm-' is second order in that species and close to first order in iodide. The Raman intensity data are not accurate enough to determine if an iodide-independent term is present in the latter case: however, if such a term exists, it is small.

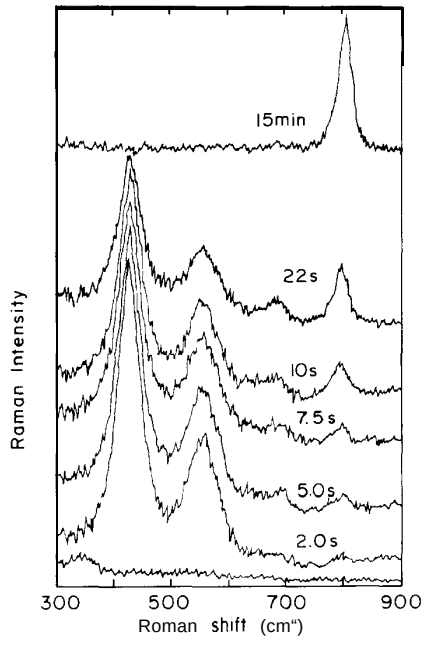

FIG. 1. Raman spectra as a function of time after reacting an I_2 (0.1 mol dm^{-3})/I^- (0.6 mol dm^{-3}) solution with an equal volume of a 2.0 mol dm^{-3} NaOH solution. 'The bottom spectrum is for the unreacted I_2'- solution.

The effect of ionic strength was studied by adding 1.4 and 0.2 mol dm^{-3} NaCl to the I_2/I^- solutions. No significant change was observed in the I_{560}/I_{430} ratio or in the time behaviour of any of the four Raman bands.

Reaction of HOCl/OCl^- with I^- at pH values of 12 and 10.5

The kinetics of iodine disproportionation were also studied at lower pH values using reaction [3]. The reactions at pH values of 12 and 10.5 were initiated by mixing 0.10 mol dm^{-3} HOC1 with an equal volume of 0.10 mol dm^{-3} NaI. At a pH of 12, the results were similar to those observed from the reaction of I_2/I^- in 1 mol dm^{-3} NaOH (reaction [2]). Two bands, at 430 ± 2 and 575 ± 5 cm-^{1}, were seen immediately after mixing, and were then the only detectable spectral features. Two additional bands appeared at 685 ± 2 and 800 ± 2 cm^{-1} after a few seconds of reaction time. The intensities of the four bands as a function of time followed a pattern similar to that observed in 1.0 mol dm^{-3}

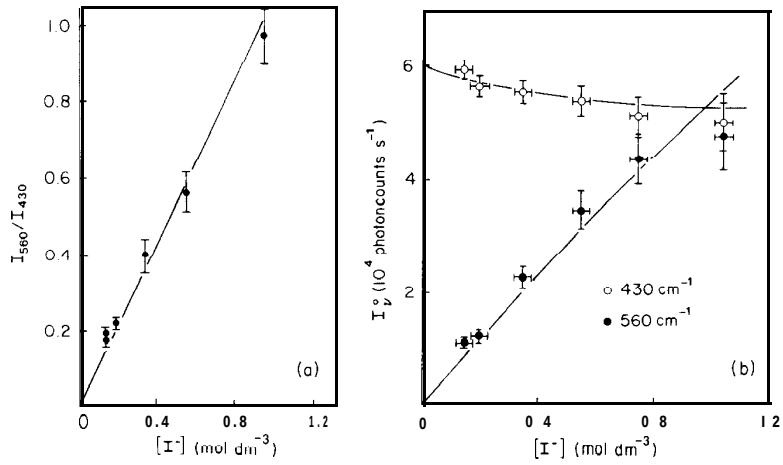

FIG. 2. (a) Ratio of the Raman intensity at 560 cm^{-1} to the Raman intensity at 430 cm-', and (b) Raman intensities at mixing time at 560 and 430 cm-', as a function of the iodide ion concentration, after reacting an I_2 (0. I mol dm^{-3})/I^- solution with an equal volume of a 2.0 mol dm^{-3} NaOH solution. The solid lines in (b) are calculated results from equilibrium [7] and the determined K_1, α_{430}, and α_{560} values.

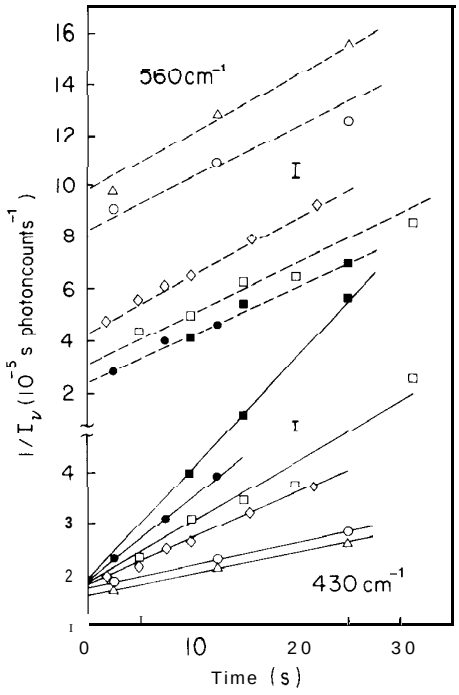

FIG 3. Second-order plots for the decay of the Raman intensities at 560 and 430 cm^{-1} for various iodide ion concentrations. The reaction was initiated by reacting I_2 (0. I mol dm^{-3})/I^- solutions with an equal volume of a 2.0 mol dm^{-3} NaOH solution. The I^- concentrations were A 0.20, ○ 0.40, ◇ 0 60, □ 1 0 ● 1 4, and ■ 2 0 mol dm^{-3}.

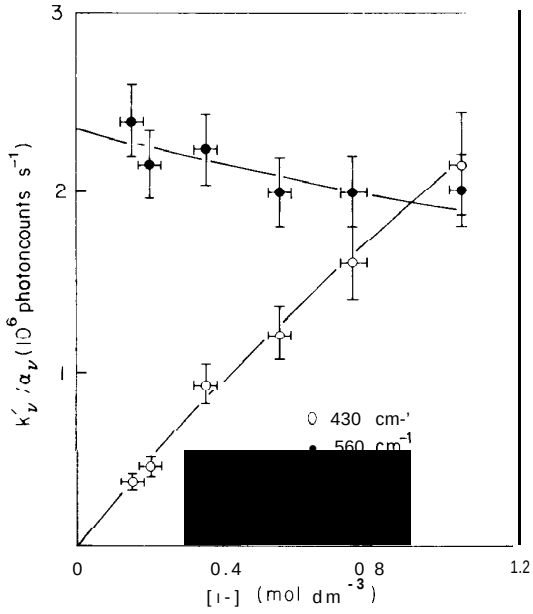

FIG. 4. Apparent second-order rate constants, divided by the Raman scattering probability, for the 430- and 560-cm^{-1} Raman bands, as a function of the iodide ion concentration.

NaOH using reaction [2]. No I_2 or I_3^- peak was observed during the course of the reaction. The differences observed at a pH of 12, compared with reaction [2] in 1 mol dm^{-3} NaOH, were (I) the band previously observed at 560 cm^{-1} shifted to 575 cm-', (2) the ratio (I_{575}/I_{430}) was smaller than that observed for all I^- concentrations studied (0.15 to 1.05 mol dm^{-3}) in 1 mol dm^{-3} NaOH, and (3) the reaction was faster than the reaction observed in 1 mol dm^{-3} NaOH for comparable I^- concentrations.

At a pH of 10.5, the Raman spectrum became simpler. The band at 430 ± 2 cm^{-1} was still present immediately after mixing, but no band was observed around 560 cm-' or around 685 cm^{-1} during the course of the reaction. The intensity of the 430-cm^{-1} band decreased with time to zero. A band at 800 cm-' appeared within a very short reaction time, increased steadily in intensity with time, and was the only band present at long reaction time. The reaction was much faster than at higher pH values. In addition to the transient iodine bands, an I_3^- band at 110 ± 2 cm^{-1} was also observed. The intensity of the I_3^- band increased from zero at mixing time, went through a maximum, then decayed back to zero at long reaction time. The maximum I_3^- concentration observed was 6.0 ± 5.0 × 10^{-3} mol dm^{-3}. It

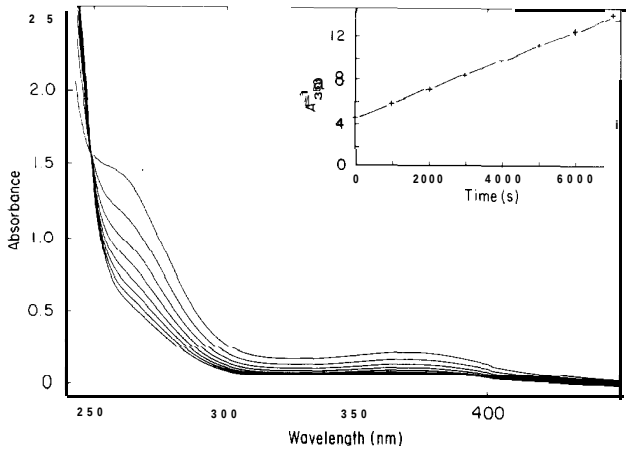

FIG. 5. Ultraviolet-visible spectra obtained as a function of time after reacting an ICl_2^- solution with a NaOH solution. The ICI; and NaOH concentrations were, after mixing, 5 X 10^{-3} and 1 mol dm^{-3}, respectively. Arrows indicate the direction the absorbance moved with time. The insert is a second-order plot of the absorbance at 363 nm.

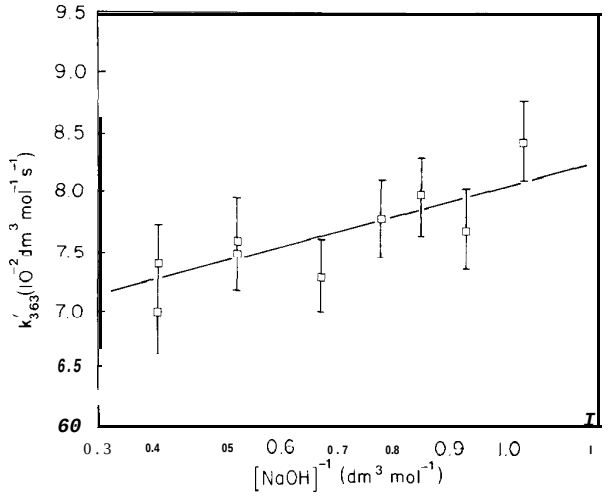

FIG. 6. Apparent second-order rate constant for the decay of IO^- at 363 nm as a function of the reciprocal NaOH concentration. Conditions were the same as those of Fig. 5, except that the NaOH concentration was varied.

was not possible to study the reaction at lower pH values using Raman spectroscopy due to the rapid increase in the rate on lowering the pH.

Ultraviolet-visible spectrophotometry

Reaction of ICl with NaOH

Figure 5 shows a series of uv-visible spectra obtained as a function of time using reaction [4]. The spectrum obtained at times close to mixing is due to the hypoiodite ion, IO^- (14). The spectra as a function of time display an isobestic point at 248 ± 1 nm with the absorbance decreasing with time at wavelengths greater than 248 nm and increasing with time at wavelengths less than 248 nm.

Plots of the inverse of the absorbance at 363 nm, A_{363}^{-1}, as a function of reaction time for various NaOH concentrations showed linear relationships, indicating that the species responsible for the light absorption at 363 nm, IO-, is decaying by a second-order process. In that case, the slopes are k'_{363}/ϵ_{363} and the intercepts are $(\epsilon_{363}C_0)^{-1}$, where k'_{363} is the apparent second-order rate constant, ϵ_{363} is the molar absorptivity at 363 nm, and C_0 is the initial concentration of the reacting species, IO^-. From the intercepts and the known initial concentrations of IO-, the molar absorptivity at 363 nm, ϵ_{363}, was found to be 60 ± 3 dm^3 mol^{-1} cm^{-1}, in agreement with the value reported previously (14). A plot of k'_{363} against the inverse of the NaOH concentration (see Fig. 6) or against the inverse of the square of the NaOH concentration is linear, whereas a plot of k'_{363} against the NaOH concentration displays a curvature. Thus, it appears that the rate of decay of the hypoiodite ion is second order in IO-, and either inverse first order or inverse second order in OH-. Iodate was found to retard the reaction both at high and at low NaOH concentration, with the reaction remaining second order. This effect has also been noted by Haimovich and Treinin (6).

Reaction of I_2/I^- with NaOH

Ultraviolet-visible spectra obtained using reaction [2] were very similar to the ones in Fig. 5 at wavelengths close to 360 nm. A plot of A_{363}^{-1} against time was also linear. giving an apparent second-order rate constant of (8.5 ± 0.8) X 10^{-2} dm^3 mol^{-1} s^{-1}, in good agreement with the value obtained above (Fig. 6) for the same NaOH concentration.

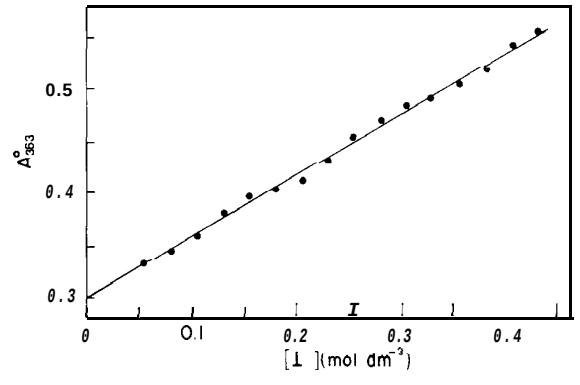

FIG. 7. Absorbance at mixing time at 363 nm as a function of the iodide ion concentration, after reacting an I_2 (5 X 10^{-3} mol dm^{-3})/I^- solution with an equal volume of a 2 0 mol dm^{-3} NaOH solution,

Varying the initial iodide concentration between 0.1 and 0.8 mol dm^{-3} for a fixed concentration of I_2 of 1 X 10^{-2} mol dm^{-3} and a fixed NaOH concentration of 1 mol dm^{-3} affected the uv-visible spectra and their time behaviour. The absorbance at 363 nm at the time of mixing, A^0_{363}, increased linearly with the iodide concentration (see Fig. 7). After an initial transient, plots of A_{363}^{-1} against time were linear (see Fig. 8), indicating that the light-absorbing species decay by a second-order process after an initial transient.

Iodide-specific electrode measurements

Reaction of ICI with NaOH

The iodide concentration, monitored using an iodide-specific electrode for reaction [4], is shown in Fig. 9(*a*). The iodide concentration increased steadily with time from zero to 3.2 ± 0.1 X 10^{-3} mol dm^{-3} at long reaction time. A comparison of the concentration of IO- as a function of time from Fig. 5 and of the' concentration of I^- as a function of time from Fig. 9(*a*) shows that the ratio $\Delta[IO^-]/\Delta[I^-]$ is 1.5 ± 0.1 for any given time interval. This confirms that the reaction is a

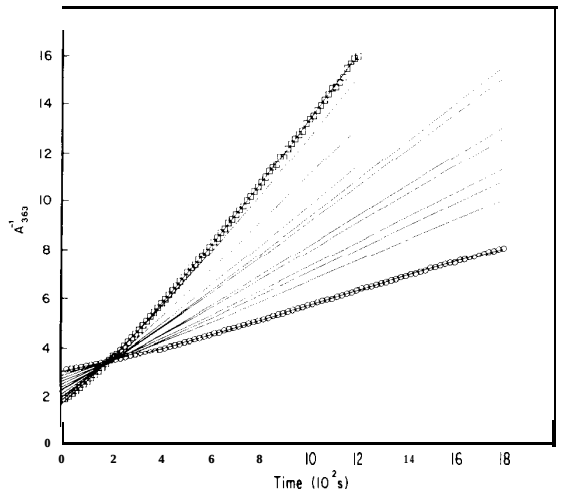

FIG. 8. Second-order plots for the decay of the absorbance at 363 nm for various iodide ion concentrations. The reaction was initiated by reacting an I_2 (5×10^{-3} mol dm^{-3})/I^- solution with an equal volume of a 2.0 mol dm^{-3} NaOH solution. For clarity, only alternate data points are indicated for the highest (□ 0.48 mol dm^{-3}) and the lowest (0 0.05 mol dm^{-3}) I^- concentration.

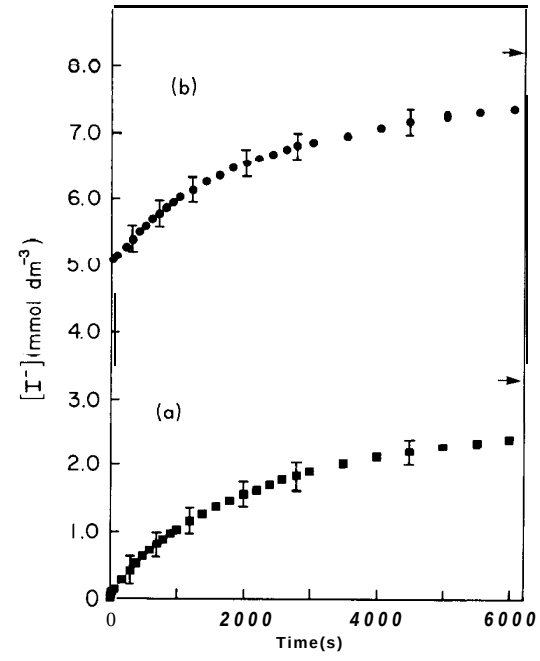

FIG. 9. Iodide ion concentration as a function of time after reacting (a), ■: an ICl_2^- solution with a NaOH solution. The concentrations of ICl_2^- and NaOH, after mixing, were 5×10^{-3} and 1 mol dm^{-3}, respectively, and (*b*), ● : a 10^{-2} mol dm^{-3} I_2 solution with an equal volume of a 2 mol dm^{-3} NaOH solution. Arrows indicate final concentrations after 48 h.

disproportionation and has the overall stoichiometry

[6] $3IO^- \rightarrow 2I^- + IO_3^-$;

From the constancy of the above ratio and the presence of an isobestic point in the uv-visible spectra (see Fig. 5), any intermediate species besides IO^-, I^-, and IO_3^- must comprise less than 5% of the total iodine in solution at any given time.

Reaction I_2 with NaOH

Reaction [2] was also monitored using the iodide-specific electrode (see Fig. 9(b)). The concentration of I very rapidly reached a value equal to the initial I_2 concentration and then increased slowly with time to a limiting value equal to 1.67 times the initial I_2 concentration. This is consistent the known stoichiometry of the overall reaction [1], and with the first step of the reaction being a rapid disproportionation of elemental iodine to the + 1 and − 1 oxidation states.

IV. Discussion

Raman spectroscopy

Kinetic analysis

The kinetic analysis of the reactions of I_2/I^- in 1 mol dm^{-3} NaOH (reaction [2]) will be considered first. The behaviour of the 685- and 800-cm^{-1} bands as a function of time, and the behaviour of the 430- and 560-cm^{-1} bands as a function of time and as a function of the iodide ion concentration, indicate that these four Raman bands belong to four different species. The band at 800 cm-' can be unambiguously assigned to IO_3^- (15). The final IO_3^- concentration was determined hy comparing the Raman intensities with that of standard $NaIO_3$ solutions. For the reactions of solutions 0.05 mol dm^{-3} in I_2 and from 0.1 to 1 mol dm^{-3} in I^- with 1 mol dm^{-3} NaOH, the final concentration of IO_3^- was 0.017 ± 0.002 mol dm^{-3} in all cases. This is consistent with the known stoichiometry of the overall reaction [1], the equilibrium being completely to the right at this low H^+ concentration. The assignment of the bands observed at 430, 560, and 685 cm^{-1} will be discussed later, after analysis of their time and iodide-concentration dependence.

The behaviour of the 560- and 430-cm-' bands as a function nf $[I^-]$, (see Fig. 2(n)) and as a function of time (see Fig. 3), suggests that these bands are due to two molecules participating in a rapidly established equilibrium involving I-:

[7] $P_{430} + iI^- \rightleftharpoons qQ_{560}$

where P_{430} and Q_{560} represent species responsible for the 430- and 560-cm^{-1} bands. Equilibrium [7] implies that the ratio $(I_{560}\alpha_{560})^q/(I_{430}\alpha_{430}[I^-]^i)$ is a constant Various combinations of q and i were explored. However, only a plot of I_{560}/I_{430} against the iodide concentration gives a straight line (see Fig. *2(a)*), indicating that the coefficients q and i are unity.

The equilibrium quotient, K_7, can be calculated from the Raman data as follows. Immediately after mixing, only P_{430} and Q_{560} are present. Extrapolation of the Raman intensities at mixing time to zero [I-] (Fig. *2(b)*) gives values of 0 and 5.9 ± 0.1 × 10' photon counts for I^0_{560} and I^0_{430}, respectively, Since the initial I_2 concentration is 0.05 mol dm^{-3}. α_{430} is found to be 1.2 ± 0.1 × 10^6 photon counts dm^3 mol^{-1} under the experimental cnnditinns used here. The value of α_{560} can then be easily obtained at each [I-] from mass balance considerations. An average value of 5.5 ± 0.5 x 10^6 photon counts dm^3 mol^{-1} was found for α_{560}. From the slope of the I_{560}/I_{430} vs. $[I^-]$ plot (Fig. 2(*a*)), a value of 0.24 ± 0.07 dm^3 mol^{-1} is obtained for K_7.

The rapidly established equilibrium between P_{430} and Q_{560} has to be considered in the calculation of the rate constants. Since the mixture is ultimately converted to iodate via a second-order process, the rate law can be written as

[8] $$-\frac{d([P_{430}] + [Q_{560}])}{dt} = k_{obs}([P_{430}] + [Q_{560}])^2$$

[9] $$k_{obs} = \sum_i k_i f_i^2$$

TABLE 1. Observed rate constants, k_{obs}, determined from the values of k'_ν obtained using Raman spectroscopy

$[I^-]$/mol dm^{-3}	k_{obs} from k'_{430}	k_{obs} from k'_{560}
0.15	0.41	0.46
0.20	0.52	0.54
0.35	1.02	0.96
0.55	1.27	1.28
0.75	1.63	1.68
1.05	2.06	2.21

where k_i is the actual rate constant for the reaction of the species i and f_i is the fraction of the total iodine concentration for each of the reactive species. In that case, k_{obs} should be related to the apparent rate constants, k'_ν, presented in Fig. 4, by

$$[10]\quad k_{obs} = k'_{560}\left(\frac{K_7[I^-]}{1 + K_7[I^-]}\right)$$

$$[11]\quad k_{obs} = k'_{430}\left(\frac{1}{1 + K_7[I^-]}\right)$$

The k_{obs} values determined from both k'_{560} and k'_{430} values are given in Table 1 as a function of [I-], and are in good agreement. The k_{obs} increases with an increase in $[I^-]$. These observed rate constants can be used to determine the actual rate constants, k_i, from eq. [9]. If P_{430} was the only reactive species, k_{obs} would be proportional to

$$\left(\frac{1}{1 + K_7[I^-]}\right)^2$$

since $f_{P_{430}}$ is given by

$$\left(\frac{1}{1 + K_7[I^-]}\right)$$

If Q_{560} was the only reactive species, then k_{obs} would be proportional to

$$\left(\frac{K_7[I^-]}{1 + K_7[I^-]}\right)^2$$

since $f_{P_{430}}$ is given by

$$\left(\frac{K_7[I^-]}{1 + K_7[I^-]}\right)$$

These were not found tn he the case. However, as can be seen from Fig. 10, a linear relationship is obtained for

$$[12]\quad k_{obs} = \frac{k_{PQ}K_7[I^-]}{(1 + K_7[I^-])^2}$$

indicating that P_{430} and Q_{560} are reacting together according to the rate equation

$$[13]\quad \frac{d}{dt}([P_{430}] + [Q_{560}]) = -k_{PQ}[P_{430}][Q_{560}]$$

with k_{PQ} having a value of 13 ± 1 dm^3 mol^{-1} s^{-1}, which was obtained from the slope in Fig. 10.

The Raman band at 685 cm-' displays a kinetic behaviour typical of a species being formed in an earlier reaction step and destroyed in a subsequent step. This species, R_{685}, is likely the product of the reaction between P_{430} and Q_{560} discussed above, and can itself react to produce iodate. If R_{685} reacts with itself

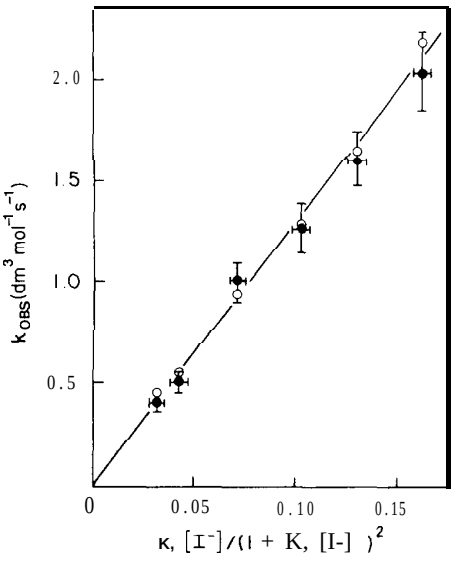

FIG. 10. Correlation of the observed rate constants with the iodide ion concentration for the Raman results in 1 mol dm^{-3} NaOH solutions.

in either a first-order or a second-order reaction, then the final IO_3^- concentration should be $(1/2)([P_{430}]^0 + [Q_{560}]^0)$ or $(1/4)([P_{430}]^0 + [Q_{560}]^0)$, respectively, where $([P_{430}]^0 + [Q_{560}]^0) = 0.05$ mol dm^{-3}. However, rhe final IO_3^- concentration was $1.7 \pm 0.2 \times 10^{-2}$ mol dm^{-3} in all cases, which is $(1/3)([P_{430}]^0 + [Q_{560}]^0)$. If R_{685} reacts with P_{430} and/or Q_{560} to form iodate, then the final concentration of iodate would be 1.67×10^{-2} mol dm^{-3}, which is in agreement with the experimental results. The mass balance at any given time after reacting the I_2/I^- solutions with the OH- solution would then be

$$[14]\quad [P_{430}]_t + [Q_{560}]_t + 2[R_{685}]_t + 3[IO_3^-]_t = [I_2]_{t=0} = 0.05 \text{ mol dm}^{-3}$$

The observed Raman intensities of the four species at any given reaction time can be used to calculate α_{685} from the above mass balance equation and the known values of α_{430} and α_{560}. If the proposed mechanism is correct, then α_{685} obtained at any given reaction time and for any given [I-] should be constant. The value of α_{685} was found to be in the range (6.6 to 6.9) $\times 10^5$ photon counts dm^3 mol^{-1}, which supports the proposed mechanism. The possibility of forming more than one molecule of R_{685} by reacting P_{430} and Q_{560} can also be rejected on the basis of mass balance

The Raman results obtained at lower pH values using reaction [3] cannot be directly compared with the results obtained from reaction [2] in 1.0 mol dm^{-3} NaOH. In reaction [3], the I^- concenrrarion is negligible at the time of mining, but increases as the reaction proceeds, whereas the iodide concentration in the reaction of I_2/I^- in 1 mol dm^{-3} NaOH is nearly constant during the course of the reaction, for a given I_2/I^- solution.

Second-order plots for I_{430} at pH values of 12 and 10.5 are compared with the data obtained for the reaction of 0.05 mol dm^{-3} I_2/0.1 mol dm^{-3} I^- with 1 mol dm^{-3} NaOH in Fig. 11. The figure shows curvatures for pH values of 12 and 10.5, indicating that the iodide concentration is not constant during the reaction. Extrapolating the data to time zero at both

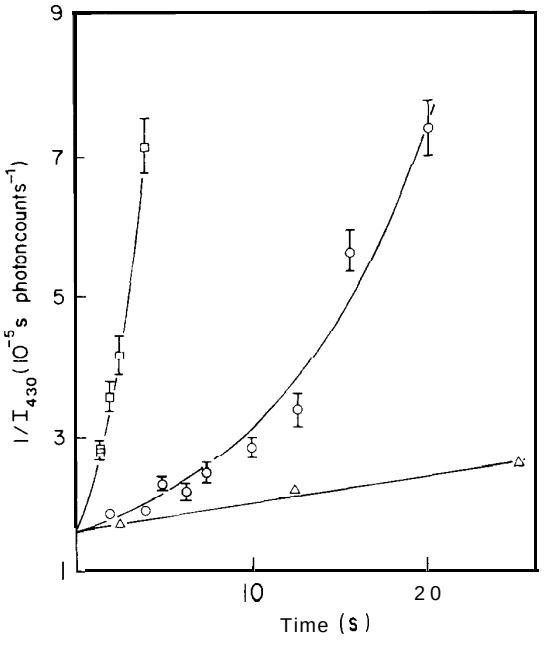

FIG. 11. Second-order plots for the decay of the Raman intensity at 430 cm^{-1} at pH values of 10.5 (Cl) and 12.0 (0), reaction [3]; and by reacting an I_2 (0.1 mol dm^{-3})/I^- (0.2 mol dm^{-3}) solution with an equal volume of a 2 mol dm^{-3} NaOH solution (△), reaction [?]

pH values gives an I^0_{430} value of 6.1 ± 0.2 × 10^4 photon counts. This corresponds to $[P_{430}]^0$ = 0.051 ± 0.002 mol dm^{-3} using the α_{430} determined from the data observed using reaction [2]. This indicates that the band observed at 430 cm^{-1} at pH values of 12 and 10.5 belongs to the same species responsible for the 430-cm^{-1} band observed using reaction [2] in 1 mol dm^{-3} NaOH, and that the iodide concentration at the time of mixing is negligible, as expected from reaction [3].

Assignment of Raman bands

The assignment of the band observed at 800 cm^{-1} to the symmetric stretching vibration of IO_3^- (symmetry *A,)* is quite obvious, as stated earlier. We assign the band observed at 685 cm^{-1} to the symmetric stretching vibration of IO_2^- We were unable to find any report in the literature on the Raman spectrum of IO_2^-. However, the Raman spectra of the corresponding chlorine and bromine compounds have been reported. The totally symmetric stretching vibration in ClO_2^- has been observed at 786 cm^{-1} by Tasaka and Toja (16). For BrO_2^-, this vibration has been assigned to the Raman band seen at 7 10 cm-' by Sombret and Wallart (17) and Evans and Lo (18).

The assignment of the remaining two bands at 560 and 430 cm^{-1} is not so straightforward. These bands are most likely due tn IO^- and I_2O^{2-} (or I_2OH^-). In 1 mol dm^{-3} NaOH solution, the equilibrium, HOI $\rightleftharpoons H^+ + IO^-$, is completely to the right. Thus, we will only consider the IO^- contribution in the following analysis. We first attempted to assign the 560-cm^{-1} band to IO^-, based on the literature assignment for the I-O stretch in HOI (the parent acid for the IO^- ion) at 572 cm^{-1} (19-22). Here it should be mentioned that the vibrational (infrared) spectrum for HOI has been reported only tor molecules isolated and produced in solid N_2 or Ar matrices. The change in the I-O vibration frequency from 572 to 560 cm-'in going from the matrix isolated acid state (HOI) to the solution state (IO-) also seemed typical of that observed for similar halogen systems: ν_{XO} in HOCl and ClO^- is 729 (23) and 713 cm- ' (16), and in HOBr and BrO^-, it is 626 (23) and 620 cm-' (17), respectively. Although the assignment of the 560-cm^{-1} band to IO- stretch would be consistent with the literature assignment for HOI, it makes it very difficult to explain the $[I^-]$ concentration dependence of relative Ramap intensities at 560 and 430 cm^{-1} described above, as well as the uv-visible data and ion-specific electrode data. We were unable to arrive at a plausible mechanism that would assign the 560-cm^{-1} band to IO^- and the 430-cm-' band to I_2O^{2-} (or I_2OH^-) and still explain the fact that the I_{560}/I_{430} ratio increases with an increase in iodide ion concentration. I hus, we have assigned the 430-cm-' band to the IO^- stretching vibration and the 560-cm-' band to the I-O stretching vibration in I_2O^{2-} (or I_2OH^-), to explain the intensity dependence on $[I^-]$. The assignment of the Raman band observed at 430 cm-' to IO^- is also supported by the Raman spectra observed using reaction [3]. The reaction of HOCl with I^- is known to produce IO^- (14) and, as there is no excess I^- ions at short reaction times, the observed band at 430cm $^{-1}$ should be assigned to IO^- rather than I_2O^{2-} (or I_2OH^-).

The assignment suggested above implies that the I-O bond is much weaker for IO^- in aqueous alkaline solution than for HOI in inert matrices. One plausible explanation for this may be found in the description of similar systems by Pimentel (24). He suggested that species isoelectronic with X^- (i.e., OH^-) can combine with groups of electronic character similar to X_2 (i.e., IO^-), where X represents a halogen. According to the above, IO^- in alkaline solution may exist as

[15] $HO^- + IO^- \rightleftharpoons [HO\text{---}IO]^{2-}$

The assignment of the I-O stretching vibration to a higher frequency for I_2O^{2-} than that for IO^- may seem unusual at first glance, yet it is not without precedent. The Cl—O stretching vibration has been assigned to a higher frequency for ClClO (962 cm-') and FClO (1038 cm^{-1}) than for Cl0 (850 cm-') by Chi and Andrews (25). These authors attributed the increase in the "Cl-O bond strength" in going from Cl0 to ClClO or FClO to the removal of the antibonding electron density from ClO, leaving a stronger Cl-O bond. A similar effect can also explain the increase in the I-O stretching vibration frequency in going from IO- to $[IIO]^{2-}$. In solutions containing iodide ions, I^- may combine with IO^- ions to form I_2OH^-:

[16] $I^- + IO^- + [I\text{---}IO]^- \xrightarrow{H^+} [I_2OH]^-$

The I_2OH^- would be a linear molecule, in agreement with the simple molecular orbital treatment of the bonding in the trihalide ions by Pimentel (24), which led him to predict that the hydroxide ion should be able to combine with I_2 to form I_2OH^-. Anbar and Taube (26) also proposed that Cl_2OH^- is a possible intermediate in the exchange reaction between Cl^- and HOCl, and suggested that its structure is analogous to that of Br_3^-

The 560-cm^{-1} band shifted to 575 cm^{-1} at lower pH. We believe that the 560-cm^{-1} band is due to unprotonated I_2O^{2-}, and that the 575-cm^{-1} band is due to partially protonated I_2OH^-. This increase in frequency is consistent with a slight increase in I-O bond strength due to an overall decrease in electron density upon protonation.

Reaction mechanism

With the assignment of IO^-, I_2O^{2-} (or I_2OH^-), and IO_2^-

given to P_{430}, Q_{560}, and R_{685}, respectively, a mechanism can be proposed for the overall disproportionation of iodine in basic solutions. The rate-determining step clearly is the disproportionation of the + 1 oxidation-state species (IO^-, I_2OH^-) to iodate and iodide, since the Raman bands due to I_2 and I_3^- disappear instantaneously upon mixing with NaOH. The following mechanism is compatible with all of the Raman results and the overall stoichiometry of reaction [1].

$$[2] \quad I_2 + OH \underset{}{\overset{K_2}{\rightleftharpoons}} IO + I^- + H^+ \qquad K_2 = 1.37 \times 10^{-9}\ dm^3\ mol^{-1}\ (28j$$

$$[17] \quad I_2 + I^- \overset{K_{17}}{\rightleftharpoons} I_3^- \qquad K_{17} = 746\ dm^3\ mol^{-1}\ (29)$$

$$[18] \quad IO^- + I^- + H_2O \overset{K_{18}}{\rightleftharpoons} I_2OH^- + OH^-$$

$$[19] \quad IO + HOI + IO^- \xrightarrow{k_{19}} IO_2^- + I^- + H^+$$

$$[20] \quad IO^- + I_2OH^- \xrightarrow{k_{20}} IO_2^- + 2I^- + H^+$$

$$[21] \quad IO_2^- + IO^- \xrightarrow{k_{21}} IO_3^- + I^-$$

$$[22] \quad IO^- + I_2OH^- \xrightarrow{k_{22}} IO^- + 2I^- + H^+$$

where equilibria [2], [17], and [18] are established rapidly. The equilibrium [18] is equivalent to equilibrium [7], and thus has a value of 0.24 ± 0.07 $dm^3\ mol^{-1}$. Equilibrium [2] is almost completely to the right at this high pH; thus, the concentrations of I_2 and I_3^- are negligible after mixing with NaOH. Reaction [19] is being considered here for completeness, since it was too slow to be observed in the Raman study (i.e., $k_{19} < k_{20}$). The rate constants, k_{21} and/or k_{22}, are larger than k_{19} and k_{20}. If both k_{21} and k_{22} were smaller than k_{19} and/or k_{20}, then the second-order plots shown in Fig. 4 would display curvature, and a substantial amount of IO_2^- (R_{685}) would accumulate in solution. On the other hand, if k_{21} and/or k_{22} were much larger than k_{19} and k_{20}, virtually no R_{685} would accumulate and k_{obs} would be given by $3\,k_{19}$ or $3\,k_{20}$. Since some R_{685} accumulates, the truth is somewhere between these two extremes.

Although we did not obtain enough data at pH 12 and 10.5 to attempt a detailed analysis, some qualitative comments can be made. The reaction was faster at lower pH, which can be explained if the reaction of HOI with HOI or IO- is faster than the reaction of IO- with IO-. Also, the I_2OH^- responsible for the Raman band at 560 cm^{-1} was not observed at a pH of 10.5. At this low pH, equilibrium [2] is not completely to the right and a small amount of I_2 is present, which will react with I^- to form I_3^- according to equilibrium [17]. The values of K_{17} and K_{18} are such that only a small amount of I_2OH^- is expected at this low pH.

Ultraviolet-visible spectrophotometry and iodide-specific electrode measurements

Reaction of ICl with NaOH

The uv-visible and iodide-specific electrode results obtained at low initial iodide concentration for reaction [4] indicate that IO-, formed by the rapid hydrolysis of ICl_2^-, disproportionates to iodide and iodate at a rate that is second-order in $[IO^-]$ and either inverse first-order or inverse second-order in [OH-]. These results suggest that both HOI and IO- participate in the reaction. Since IO- and HOI are in rapid acid-base equilibrium

$$[23] \quad HOI \overset{K_{23}}{\rightleftharpoons} IO^- + H^+$$

the general rate law for the disproportionation would be

$$[24] \quad -\frac{d[IO^- + HOI]}{dt} = k_{24a}[HOI]^2 \quad k_{24b}[HOI][IO^-] + k_{24c}[IO^-]^2$$

This can be rewritten in terms of IO^- only as

$$[25] \quad -\frac{d[IO^-]}{dt} = \left[\frac{k_{24a}\frac{[H^+]^2}{K_{23}} + k_{24b}\frac{[H^+]}{K_{23}} + k_{24c}}{1 + \frac{[H^+]}{K_{23}}}\right][IO^-]^2 = k_{obs}[IO^-]^2$$

The rate constant k_{24a} is known to be approximately 200 $dm^3\ mol^{-1}\ s^{-1}$ (5). The contribution from the term in $[HOI]^2$ would thus be quite small at the [OH-] concentrations used (1 to 2.5 mol dm^{-3}) and can be neglected. The value of k_{24b} can be obtained from the slope of the plot of k_{obs} against $[NaOH]^1$ (Fig. 6) and is 40 ± 7 $dm^3\ mol^{-1}\ s^{-1}$. Not much can be said about the value of k_{24c} except that, from Fig. 6, it is estimated to be less than 7.2 × $10^{-2}\ dm^3\ mol^{-1}\ s^{-1}$.

Reaction of I_2/I^- with NaOH

The iodide-specific electrode and uv-visible spectroscopy results for reaction [2] are consistent with a rapid hydrolysis and disproportionation of elemental iodine to the + 1 and − 1 oxidation states, followed by a slower further disproportionation to iodide and iodate with the overall stoichiometry as shown in eq. [6].

For mixtures obtained by reacting I_2/I^- solutions with a NaOH solution, the absorbance at 363 nm at mixing time, A^0_{363}, increases with the initial concentration of iodide, in agreement with the observations of Sigalla (27) and Chia (28). This is likely due to the formation of other iodine compounds besides IO-, probably I_3^- formed through equilibria [2] and [17]. However, the equilibrium amounts of I_3^- cannot account entirely for the increase in absorbance at mixing time with the iodide ion concentration. An additional light-absorbing species is required.

Both Sigalla (27) and Chia (28) have proposed the involvement of equilibrium [18] in solutions containing hypoiodite and iodide. Since I_2 and I^- have no appreciable light absorption at 163 nm, from equilibria [2], [17], and [18], the absorbance at 363 nm at mixing time would be given by

$$[26] \quad A^0_{363} = \frac{C_0(\epsilon^{IO^-}_{363} + \epsilon^{I_2OH^-}_{363}K_{18}[I^-]/[OH^-] + \epsilon^{I_3^-}_{363}[I^-]^2K_{17}/K_2[OH^-]^2)}{(1 + K_{18}[I^-]/[OH^-] + [I^-]^2K_{17}/K_2[OH^-]^2 + [I^-]/K_2[OH^-]^2)}$$

where C_0 is the initial iodine concentration. Here, $\epsilon^{OI^-}_{363}$ is the specific absorptivity for IO- at 363 nm and has been determined above as being equal to 60 mol^{-1} dm" cm-'. The specific absorptivity for I_3^- at 363 nm is 19 000 $mol^{-1} dm^3$ cm-' (29).

A non-linear least-squares fit to eq. [26] was used to determine $\epsilon^{I_2OH^-}_{363}$ and K_{18} from 17 measurements of A^0_{363} as a function of I^- concentration, covering the range from 0.05 mol dm^{-3} to 0.5 mol dm^{-3}. Values of 750 ± 50 $mol^{-1}\ dm^3\ cm^{-1}$ and

0.15 ± 0.01 dm^3 mol^{-1} were obtained, respectively, and could represent the data with an average deviation of 0.6% and a maximum deviation of 1%. Inclusion of additional species having the general formula $H_zO_xI_y$ did not significantly improve the fit, and was deemed unnecessary. The equilibrium constant value agrees well with the K_{18} value calculated from the Raman results.

Although hypoiodite was the predominant form of iodine in these solutions, the equilibria with I_2, I_3^-, and I_2OH^- have to be considered in the calculation of the rate constants. The rate for each experiment was found to obey the following relation after an initial transient:

$$[27] \quad -\frac{d(\Sigma[I])}{dt} = k_{obs}(\Sigma[I])^2$$

where $\Sigma[I]$ is $([I_2] + [I_3^-] + [IO^-] + [I_2OH^-])$, and can be calculated from the absorbance at 363 nm as a function of time using the relation

$$[28] \quad \Sigma[I] = A'_{363}C_0/A^0_{363}$$

The values of k_{obs} were obtained from plots of the inverse of $\Sigma[I]$ vs. time, and are shown in Fig. 12(a). It becomes evident that at 25°C, in 1 mol dm^{-3} NaOH solution, k_{obs} can be written as

$$[29] \quad k_{obs} = k'_{29} + k''_{29}[I^-]$$

with $k'_{29} = 0.05$ dm^3 mol^{-1} s^{-1} and $k''_{29} = 2.60$ dm^3 mol^{-1}s^{-1}.

Since at zero iodide ion concentration only IO^-, and very small amounts of I_3^- and I_2, are present, the first term, k'_{29}, should be equivalent to $k_{24c} + k_{24b}[H^+]/K_{23}$, as can be seen from eq. [25]. The second term would be expected to be composed of a combination of the four equilibrium iodine species, as given in eq. [9] in generalized form. If IO- was the only reactive species, then the observed rate constant would decrease with an increase in [II]. If I_2OH^- was the only reactive species, then k_{obs} would be given by

$$[30] \quad k_{obs} = k'_{29} + k_{(I_2OH^-)}f^2_{I_2OH} = k'_{29} + k_{(I_2OH^-)}\left[\frac{1}{1 + [OH^-]/K_{18}[I^-] + K_{17}[I^-][H^+]/K_{18}K_2 + [H^+]/K_{18}K_2}\right]^2$$

where $f_{I_2OH^-}$ can be determined from equilibria [2], [17], and [18]. The terms $K_{17}[I^-][H^+]/K_{18}K_2$ and $[H^+]/K_{18}K_2$ are small. Therefore, $(k_{obs} - k'_{29})$ would be proportional to

$$\left(\frac{1}{1 + 1/K_{18}[I^-]}\right)^2$$

This was not found to be the case. Since neither of these attempts to correlate the data with a single reactive species was successful, various combinations of I_3^-, I_2, IO-, and I_2OH^- were considered.

Assuming that IO^- and I_2OH^- are reacting together, a linear correlation was obtained for

$$[31] \quad k_{obs} = \frac{k_{IO^-,I_2OH^-}K_{18}[I^-]}{(1 + K_{18}[I^-])^2} + k'$$

as shown in Fig. 12(b). From the slope of the line in this figure and the K_{18} values determined above, k_{IO^-,I_2OH^-} is equal to 19.5 ± 0.05 dm^3 mol^{-1} s^{-1}. The rate law can be rewritten as

$$[32] \quad -\frac{d}{dt}([I_2] + [I_3^-] + [IO^-] + [I_2OH^-]) = 0.05[IO^-]^2 + 19.5[IO^-][I_2OH^-]$$

and is valid for 25°C and in 1 mol dm^{-3} NaOH.

Both the rate expression and the value of k_{IO^-,I_2OH^-} are entirely compatible with the mechanism proposed to explain the Raman results (eqs. [2], [17]–[22]). The iodide-independent term is quite small and was not detectable in the Raman experiments, since relatively high concentrations of I^- were required to dissolve a sufficient amount of I_2. According to the uv-visible results, k_{21} and/or k_{22} is larger than k_{19} and k_{20} in eqs. [19]–[22], but not immensely so. It k_{21} or k_{22} was much larger than k_{20}, then the plots of $(\Sigma[I])^{-1}$ against time would be linear with slopes of $3k_{19}[I^-]/K_{18}$. Since a curvature is observed at short reaction times, k_{21} and/or k_{22} are somewhat larger than k_{19}.

The differential equations resulting from this mechanism were integrated numerically, using a modified Gear algorithm (30). The values of k_{20}, k_{21}, and k_{22} were obtained by using a non-linear least-squares routine incorporating Marquat's algorithm (31). The objective function was the absorbance of the solutions at 363 nm as a function of time and iodide concentration:

$$[33] \quad A'_{363} = \epsilon^{IO^-}_{363}[IO^-]_t + \epsilon^{I_2OH}_{363}[I_2OH^-]_t + \epsilon^{I_3^-}_{363}[I_3^-]_t$$

where the various concentrations as a function of time were from the numerical integration, assuming that equilibrium between I;, I_2, IO-, and I_2OH^- is achieved rapidly. Values of 6.0 ± 0.2, 0.5 ± 0.1, and 26 ± 2 dm^3 mol^{-1} s^{-1} were obtained for k_{20}, k_{21}, and k_{22}, respectively.

Thus, the Raman and the uv–visible spectrophotometric results can be interpreted in terms of a common mechanism. The Raman results provide an unambiguous identification of the species involved, whereas the uv-visible results provide accurate values of the rate constants. It appears that, if the concentration of iodide ions is above 5×10^{-2} mol dm^{-3}, in 1 mol dm^{-3} NaOH, the disproportionation of hypoiodite occurs preferentially through I_2OH^-.

Comparison with the literature

The formation of a weak complex between IO^- and I^- has been proposed in the past by Sigalla (27) and also by Chia (28) to explain the dependence of the uv-visible absorbance of IO^- solutions on the concentration of iodide ions. Chia reported a value of 0.13 for K_{18} at 25°C, whereas Sigalla reported a value of 3×10^{-2} for K_{18} at 25°C, after correction for ionic strength effects. The origin of the discrepancy is unclear. In Chia's experiments, IO^- and I_2OH^- were the dominant species in solution. Due to the large specific absorptivity of I_3^-, these three species contributed to the absorbance in similar proportions. Thus, Chia observed a larger than expected increase in absorbance with an increase in iodide ion concentration. In Sigalla's experiments, I_3^-, IO^-, and I_2OH^- were present in similar proportions. Due to the large specific absorptivity of I_3^-, this species was the only one contributing significantly to the absorbance, and Sigalla observed a lower than expected

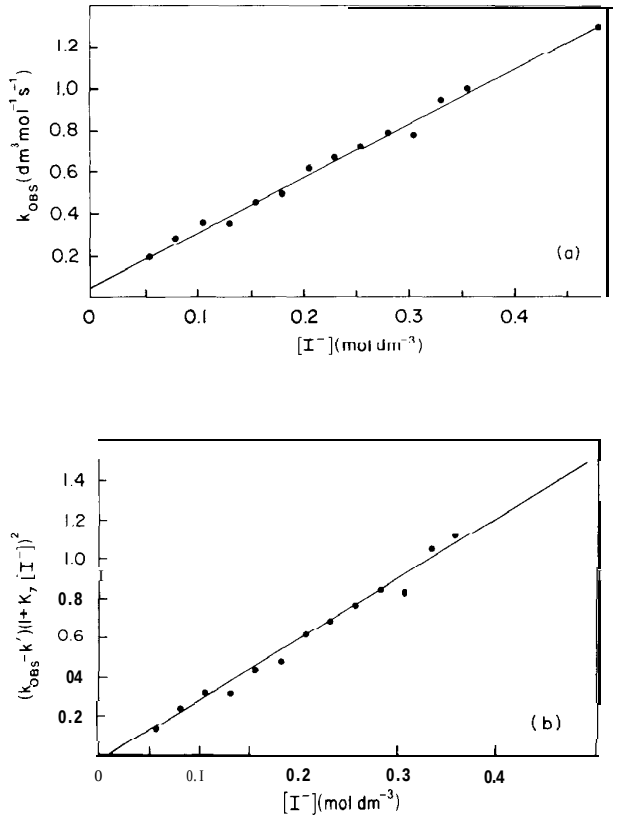

FIG. 12. For the reaction of Fig. 8, (a) observed rate constants for the decay of A_{363} as a function of [I-], and (b) correlation of the rate constants with [I-].

increase in absorbance as the iodide ion concentration was increased. Our experimental conditions were similar to Chia's and our value for $_{18}$ is in reasonable agreement with hers.

Li and White (8) have obtained, using a titration technique, the following rate law for the decomposition of hypoiodite in basic solutions:

$$[34] \quad -\frac{d[IO^-]}{dt} = k_r[IO^-]^2 + k_s\frac{[IO^-]^2[I^-]}{[OH^-]}$$

with k_r having a value of 5 X 10^{-2} dm^3 mol^{-1} s^{-1} and k_s having a value of 2.18 dm^3 mol^{-1} s^{-1}. Forster (11) and Skrabal (10) also concluded, using a titration technique, that the rate of reaction at high concentrations of OH- and I$^-$ ions is proportional to the concentration of IO- and I$^-$ inns, although they failed to detect the small I--independent term. Forster (11) found a value of 1.2 for the rate constant k_s, whereas Skrabal (10) reported a value of 1.45. The second term of our rate law and our k''_{29} value of 2.60 dm^3 mol^{-1} s^{-1} agree with the results of these earlier studies.

In later experiments, in the presence of silver oxide and silver iodide, Skrabal and Hohlbaum (9) obtained evidence that the first term of the rate law at 25°C is

$$[35] \quad -\frac{d[IO^-]}{dt} \quad \theta.03\frac{[IO^-]^2}{[OH^-]}$$

although Li and White (8) argued against a reciprocal (OH-] dependence. Our results at low [I-], obtained using reaction

TABLE 2. Rate constants for the disproportionation of the hypohalites at 25°C, in dm^3 mol^{-1} s^{-1}

X	k		X$^-$ effect
	$XO^- + XO^-$	$XO^- + XO_2^-$	
Cl"	1.1 × 10^{-8}	1.8 x 10^{-6}	None
Br^b	1.0 × 10^{-6}	1.5 x 10^{-5}	Slight positive
I'	<7 x 10^{-2}	0.5	Marked positive

"Value from ref. 32.
'Value from ref. 33.
'Value from this work.

[2], indicate that the iodide-independent part of the rate law consists of two terms:

$$[36] \quad -\frac{d[IO^-]}{dt} = a[IO^-]^2 + b\frac{[IO^-]^2}{[OH^-]}$$

where a is less than 7 × 10^{-2} dm^3 mol^{-1} s^{-1} and b is 2 × 10^{-2} dm^3 mol^{-1} s^{-1}. This seems to reconcile the Li and White (8) and Skrabal and Hohlbaum (9) data.

Haimovich and Treinin (6) have also studied the decomposition of hypoiodite in alkaline solutions at low iodide ion concentrations. They reported a value nf (4.0 ± 0.4) X 10^{-2} dm^3 mol^{-1} s^{-1} for the rate constant in 4 mol dm^{-3} NaOH, and a value of (2.7 ± 0.2) X 10^{-2} dm^3 mol^{-1} s^{-1} in 6 mol dm^{-3} NaOH, which leads to a value of 2 × 10^{-2} dm^3 mol^{-1} s^{-1} for the [OH]$^{-1}$-dependent term, in good agreement with our b value. They also noted that, for I$^-$ concentrations less than 8 × 10^{-2} mol dm^{-3}, no effect on the rate could be detected and that, on further raising [I], the rate increased. This is in qualitative agreement with our observations.

The mechanism for the conversion of hypochlorite or hypobromite to chlorate or bromate ions is well known (32, 33). The reactions consist of two steps:

$$[37] \quad XO^- + XO^- \xrightarrow{\text{slow}} XO_2^- + X^-$$

$$[38] \quad XO^- + XO_2^- \xrightarrow{\text{fast}} XO_3^- + X^-$$

with the formation of the halite ion being the rate-determining step and the subsequent formation of halate ion being rapid. The geometry of the activated complex for the first step is likely

$$[39] \quad \left[\begin{matrix} X\ldots O{-}X \\ | \\ O \end{matrix}\right]^{2-} \rightarrow \left[\begin{matrix} X{-}O \\ | \\ O \end{matrix}\right]^{-} + X^-$$

The first step is, thus, a nucleophilic displacement of one base (X^-) by another (XO^-).

Using radioactive chlorine, Anbar and Taube (26) have demonstrated that, at least in the chlorine case, the second step involves the formation of a non-symmetrical intermediate in which the chlorine atoms remain distinct, such as

$$[40] \quad \left[\begin{matrix} Cl\text{-}O\ldots & Cl\text{-}O \\ & | \\ & O \end{matrix}\right]^{2-} \rightarrow Cl^- + ClO_3^-$$

Presumably, this is also valid for the bromine system.

Our results for the iodine system indicate that the first step of iodine(I) disproportionation at high hydroxide and iodide ion concentrations consists of two parallel reactions: a slow reaction between IO- (or HOI) and IO^-, and a faster reaction between IO- (or HOI) and I_2OH^-. The slower path presumably is similar to the chlorine and bromine cases described above (reaction

[39]). The reason that the other path is more rapid can be readily explained. We suggest that IO- in aqueous solution may exist as a loosely bound complex $[HO...IO]^{2-}$ with a weakened I-O bond, while the I-O bond is strengthened in I_2OH^-. Therefore, if the activated complex and the nucleophilic displacement occur as follows,

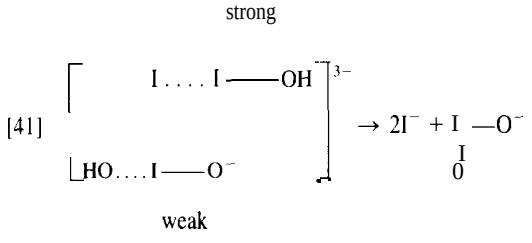

the activated complex would be more stable than that formed by HOI and $[HO..IO]^{2-}$. The second step in the disproportionation of iodine(I) also consists of two parallel reactions: a slow reaction between IO- (or HOI) and IO_2^-, and a faster reaction between I_2OH^- and IO_2^-. The slow path likely proceeds by a mechanism similar to the chlorine system (reaction [40]). The other path is more rapid, presumably for the same reasons as in the first step.

A comparison of the rates for the slower paths with the analogous bromine and chlorine reactions can be found in Table 2. The rates increase on going from hypochlorite to hypoiodite. This trend is to be expected since the electronegativity of the halogen is in the order Cl > Br > 1. This would cause the partial positive charge on the halogen to increase on going from ClO^- to IO-, favouring electrostatic interactions. However, the increase on going from the Br to I system is too large to be explained by electrostatic interaction alone. We believe that the weakened O-I bond in $[HO..IO]^{2-}$ favours a more stable activated complex for the reaction of IO- with IO^- and IO- and IO_2^-, thus increasing the rate even further.

Chloride has no effect on the rate of disproportionation of hypochlorite. Bromide slightly increases the rate of disproportionation of hypobromite, whereas iodide has a marked accelerating effect on the disproportionntion of hypoioditc. Out study indicates that the pronounced effect in the case of hypoiodite comes from the formation of the reactive species I_2OH^-, which is expected to have a structure similar to I_3^-. Since the order of stability for the trihalides IS $I_3 > Br_3^- > Cl_3^-$ (34), the relative effect of the halides on the hypohalites disproportionation can be explained if the X_2OH^- species follow the same order of stability as the trihalides.

It is tempting to try to relate our work to the complex topic of the mechanism of the Dushman reaction (reverse reaction [1]). Our experiments were performed in alkaline solutions whereas most of the studies of the Dushman reactions have been done in acidic media. This precludes quantitative calculations. However, some qualitative comments can be made.

Liebhafskv and Roe (2) have summarized the numerous studies of the Dushman' reaction. They concluded that the kinetics of the reaction are best described by a rate law of the form:

$$[42]\quad R = (k_1 \quad k_2[I^-])([H^+]^2[IO_3^-][I^-])$$

The reaction is first order in iodide at iodide concentrations below 10^{-6} mol dm^{-3} and second order in iodide at higher concentrations. The two-term rate law is accounted for by a mechanism involving the polynuclear iodine species I_2O_2 (or $H_2I_2O_3$). Liebhafsky and Roe (2) state that the existence of such a species is also needed to explain the results of Skrabal(9, 10) on the disproportionation of I_2 into IO_3^- and I^- in alkaline solution. Our study shows that the results of Skrabal can be explained by the presence of the I_2OH^- species, which we have unambiguously identified using Raman spectroscopy. Although I_2OH^- is present in significant concentration at high pH, its concentration would be quite low at low pH. In fact we could not detect any Raman signal due to this species at pH 10 and below. However, Palmer and Van Eldik (35) have recently demonstrated that I_2OH^- plays an important role in the hydrolysis of I_2 to I^- and HOI at low pH, even if it is present in very low concentration. It would be interesting to see if I_2OH^- can be substituted for I_2O_2 in the mechanism of the Dushmon reaction.

Acknowledgements

This work was funded jointly by Atomic Energy of Canada Limited and Ontario Hydro under the CANDEV agreement. The assistance of Mr. G. J. Wallace in performing some of the Raman experiments is acknowledged. The authors thank Drs. R. J. Lemire and W. C. H. Kupferschmidt of the Whiteshell Nuclear Research Establishment and Dr. D. A. Palmer of Oak Ridge National Laboratory for helpful comments on the manuscript.

1. P. P. S. SALUJA, K. S. PITZER, and R. C. PHUTELA. Can. J. Chem. 64, 1328 (1986).
2. H. A. LIEBHAFSKY and G. N. ROE. Int. J. Chem. Kinet. **11**, 693 (1979).
3. E. ABEL and F. STADLER. Z. Phvs. Chem. **22**. 49 (1926).
4. S. DUSHMAN. J. Phys. Chem. **8**. 453 (1904).
5. T. R. THOMAS, D. T. PENCE, and R. A. HASTY. J. Inorg. Nucl. Chem. 42, 183 (1980).
6. 0. HAIMOVICH and A. TREININ. J. Phys. Chem. **71**, 1941 (1967); Nature, 207, 185 (1965).
7. M. H. HASHMI, A. A. AYAY, A. RASHID, and E. ALI. Anal. Chem. 36, 1379 (1964).
8. C. H. LI and C. F. WHITE. J. Am. Chem. Soc. 65, 335 (1943).
9. A. SKRABAL and R. HOHLBAUM. Monatsh. Chem. 37, 191 (1916).
10. A. SKRABAL. Monatsh. Chem. **33**, 99 (1912); **32**, 185 (1911); **32**, 167 (1911).
11. E. L. C. FORSTER. J. Phys. Chem. 7, 640 (1903).
12. D. L. CASON and H. N. NEUMANN. J. Am. Chem. Soc. 83, 1822 (1961).
13. W. KIEFER and H. J. BERNSTEIN. Chem. Phys. Lett. **16**, 5 (1972).
14. J. PAQUETTE and B. L. FORD. Can. J. Chem. 63, 2444 (1985).
15. J. R. DURIG, 0. D. BONNER, and W. H. BREARZEALE. J. Phys. Chem. 69, 3886 (196.5).
16. A. TASAKA and T. TOJA. Sci. Eng. Rev. Doshisha Univ. 23. 14 (1982); Rep. Asahi Glass Found. Ind. Technol. 39, 103 (1981).
17. B. SOMBRET and F. WALLART. C. R. Acad. Sci. Paris (Ser. B). 277, 663 (1973).
18. J. C. EVANS and G. Y.-S. Lo. Inorg. Chem. 6, 1483 (1967).
19. J. F. OGILVIE, V. R. SLARES, and M. J. NEULANDS. Can. J. Chem. 53, 269 (1975).
20. J. F. OGILIVIE. Can. J. Spectrosc. **19**, 171 (1974).
21. N. WALKER, D. E. TEVAULT, and R. R. SMARDZEWSKI. J. Chem. Phys. 69, 564 (1978).
22. J. N. MURRELL, S. C. CARTER, I. M. MILLS, and M. F. GUEST. Mol. Phys. 37, 1199 (1979).
23. I. SCHWAGER and A. ARKELL. J. Am. Chem. Soc. 89, 6006 (1967).
24. G. PIMENTEL. J. Chem. Phys. **19**, 446 (1951).
25. F. K. CHI and L. ANDREWS. J. Phys. Chem. 77, 3062 (1973).

26. M. ANBAR and H. TAUBE. J. Am. Chem. Soc. **80**, 1073 (1958).
27. J. SIGALLA. J. Chim. Phys. 58, 602 (1961); Nature, 183, 178 (1959).
28. Y.-T. CHIA. Thesis, UCRL, No. 8311. 1958.
29. T. L. ALLEN and R. M. KEEFER. J. Am. Chem. Soc. 77, 2957 (1955).
30. M. B. CARVER. *In* Mathematics and computers in simulation. Vol. XXII. North-Holland Publishing Company. 1980. p. 298.
31. D. W. MARQUAT. J. Soc. Ind. Appl. Math. 11, 431 (1963).
32. M. W. LISTER. Can. J. Chem. 34,465 (1956).
33. M. W. LISTER and P. E. MCLEOD. Can. J. Chem. 49, 1987 (1971).
34. L. PAULING. The nature of the chemical bond. 3rd ed. Cornell University Press, Ithaca. 1960.
35. D. A. PALMER and R. VAN ELDIK. Inorg. Chem. 25,928 (1986).